J Appl Electrochem (2011) 41:1077–1085
DOI 10.1007/s10800-011-0331-y

ORIGINAL PAPER

Pulse current electrodeposition and corrosion properties of Ni–W alloy coatings

M. Zemanová · M. Krivosudská · M. Chovancová · V. Jorík

Received: 11 January 2011 / Accepted: 21 June 2011 / Published online: 12 July 2011

Abstract Ni–W alloy coatings were prepared on a mild steel substrate by means of pulse current (PC) and compared to the coatings electrodeposited by direct current (DC). In particular the study dealt with the influence of the frequency using pulse current on the surface morphology while maintaining a constant duty cycle. A constant charge for DC and PC electrodeposition of Ni–W alloy coatings was used. The morphology of the coatings was explored by scanning electron microscopy and the composition of the coatings was analysed by X-ray powder diffraction and energy dispersive X-ray analysis. Corrosion resistance of Ni–W alloy coatings was investigated by potentiodynamic polarization in a chloride medium. The corrosion products were analysed by Raman spectroscopy. It was found that the temperature of the electrolysis affects current efficiency of the DC and PC electrodeposition. The frequency of pulse electrodeposition alters the morphology of the Ni–W alloy coatings. There was evidence of the positive influence of increased tungstate concentration in the electrolyte on corrosion resistance of the Ni–W alloy coatings.

Keywords Ni–W alloy · Pulse plating · Electrodeposition · Morphology · Corrosion resistance

1 Introduction

Ni–W is nominated as a promising environmental friendly alloy to replace hard chromium due to the satisfactory appearance of the coating, mechanical and anti-corrosion properties. It is well known that tungsten cannot be deposited from an aqueous solution. Only anomalous co-deposition of the tungsten with the elements of the iron group allows the deposition from the aqueous solution [1]. Citric baths with a citrate compound were successfully used to obtain Ni–W alloy coatings [2–4]. The citrate compound in the electrolyte was used to improve current/Faradaic efficiency of the process and the solubility of the metal ions in the bath [5]. The complex formed during the electrodeposition makes the Ni–W alloy coatings easier to co-deposit from the baths. Generally, one can claim that the electrodeposition of Ni–W alloy coatings is sensitive to the conditions of electrodeposition e.g. substrate, composition and pH of the electrolyte [6–8]. To the best of the author's knowledge Ni–W was electrodeposited mainly on a copper substrate.

Gáliková's work [4] revealed optimal conditions concerning Ni–W alloy coatings deposition on the mild steel substrate applying direct current (DC). Ni–W alloy coatings were prepared using mild steel substrate and a charge of the process constant for both DC and PC electrodeposition. It is assumed that the usage of pulse current has a synergetic influence on the formation of Ni–W alloy coatings. Mainly active time-on time t_{on}, relaxation time-off time t_{off} and duty cycle ($t_{on}/(t_{on} + t_{off})$) are decisive parameters for PC electrodeposition.

Corrosion resistance of Ni–W is assumed as a promising quality. Yao et al. even found out that Ni–W is more corrosion resistant than the stainless steel 304 in acidic medium [9].

The aim of this work was to prepare Ni–W alloy coatings on a mild steel substrate by PC electrodeposition. The influence of electrolysis conditions and pulse parameters on the morphology of the coatings was studied. Nanocrystalline Ni–W coatings prepared by PC electrodeposition were

M. Zemanová (✉) · M. Krivosudská · M. Chovancová · V. Jorík
Department of Inorganic Technology in Bratislava, STU in Bratislava, Radlinského 9, 81237 Bratislava, Slovakia
e-mail: matilda.zemanova@stuba.sk

chosen to explore corrosion resistance of the coatings and compare them to the coatings prepared by DC electrodeposition. Corrosion resistance of Ni–W alloy coatings was investigated by applying the method of polarization resistance.

2 Experimental part

In this work, a two-electrode cell was used with parallel plate electrode configuration. A sheet of mild steel with an exposed area of 18 cm^2 was used as a cathode. A nickel sheet was used as an anode and was placed 3.7 cm away from the cathode. The system was two anodic to deposit both sides of the cathode sheet. The anode to cathode area ratio was ~ 5 high enough to prevent polarization of the anode and an increase in the voltage drop between the electrodes. Electrolytes with a tungstate concentration of 0.242 mol dm^{-3} (E1) and 0.5 mol dm^{-3} (E2), respectively, were used. The pH of the electrolyte was about 6.

Electroplating was conducted at a constant current density of 2 A dm^{-2} for DC and a constant average current density of 2 A dm^{-2} for PC keeping the charge of the process constant. The DC was controlled by HQ power supply PS 3003L (Netherlands) and the PC was controlled by pe86 (plating electronic, Germany). The constant duty cycle (9.1%) was fixed for all investigated parameters during the pulse cathodic rectangular deposition. Deposition time was 30 and 60 min, respectively, and temperature was kept constant at 60 °C by means of a water thermostat. The electroplating was realised at ambient (laboratory) temperature as well. Agitation was conducted with a glass mechanical stirrer (~ 100 rpm). A mild steel substrate with a thickness of 1 mm was used as a cathode. The preparing process for all specimens was as follows: the samples were mechanically polished with different grades of emery paper up to 1000, then degreased in a commercial solution Aktigal (ATOTECH, Germany), and subsequently activated in a 20% sulphuric acid solution (Mikrochem, Slovakia). After each operation intense rinse with laboratory water and distilled water followed.

All experiments were repeated three times to verify the reproducibility of the results.

The Faradaic/current efficiency (CE) was calculated from the charge passed, the weight gained and the chemical composition of the deposit, as determined by energy dispersive X-ray analysis (EDX) using the equation presented in the work of Eliaz et al. [2]:

$$CE = \left(w/It \left(\sum \frac{c_i n_i F}{B M_i} \right) \right) \times 100 \quad (1)$$

where w is the measured weight of the deposit (g), I is the current passed (A), t is the deposition time (h), c_i is the weight fraction of the element (either nickel or tungsten) in the binary alloy deposit, n_i is the number of electrons transferred in the reduction of 1 mol atoms of that element ($n_i = 2$ for nickel and 6 for tungsten), M_i is the atomic weight of the element (g mol^{-1}), F is the Faraday constant (96 485.3 C mol^{-1}) and B is a unit conversion factor (3600 C A^{-1} h^{-1}).

X-ray powder diffraction (XRPD) analysis was carried out with the Bragg–Brentano diffractometer Philips PW 1730/1050, using ß-filtered CoKα radiation, 40 kV/35 mA in the range of 20–100° 2Θ, step 0.02°. The crystallite size of the chosen coatings was calculated from the powder diffraction patterns using the Scherer equation [10].

Corrosion resistance of the prepared samples was measured by potentiodynamic polarization in the three-electrode system by Autolab Instruments model PGSTAT 30. The measurements were carried out in 6 wt% solution of NaCl at ambient temperature. A calomel electrode served as the reference, the counter electrode was graphite and the tested sample was a working electrode. The scan rate was 10 mV s^{-1}. Software served to determine polarization resistance and consequently to calculate the corrosion rate [11, 12].

The morphology and composition of the tested samples before and after corrosion were analysed. The morphology and the composition of the samples were investigated by SEM (Zeiss ZV 40, Germany) and by EDX (Bruker, Germany), respectively.

The Raman spectra were measured by Dilor–Jobin–Yvon–Spex spectrometer type LabRam equipped with confocal microscope Olympus BX-40 and He–Ne laser excitation (632.8 nm, 15 mW), grating monochromator (450–1.05 μm) and CCD detector with resolution higher than 1.3 cm^{-1}. The spectra were collected at 20 °C provided by air conditioning.

3 Results

3.1 Morphology study

The results of the calculated current efficiencies for *direct current* Ni–W alloy coating electrodeposition are presented in Fig. 1. One can see that higher temperature during electrodeposition positively influences the current efficiency of the process. The obtained results are in accordance with the work of Eliaz et al. [2]. The positive influence of the elevated temperature of Ni–W electrodeposition is attributed to the low overvoltage of the nickel at higher temperatures (60 °C) that can support the electrodeposition of tungsten at higher temperature as well. The current efficiency for the coatings deposited from E2 electrolyte is lower in comparison with current efficiencies

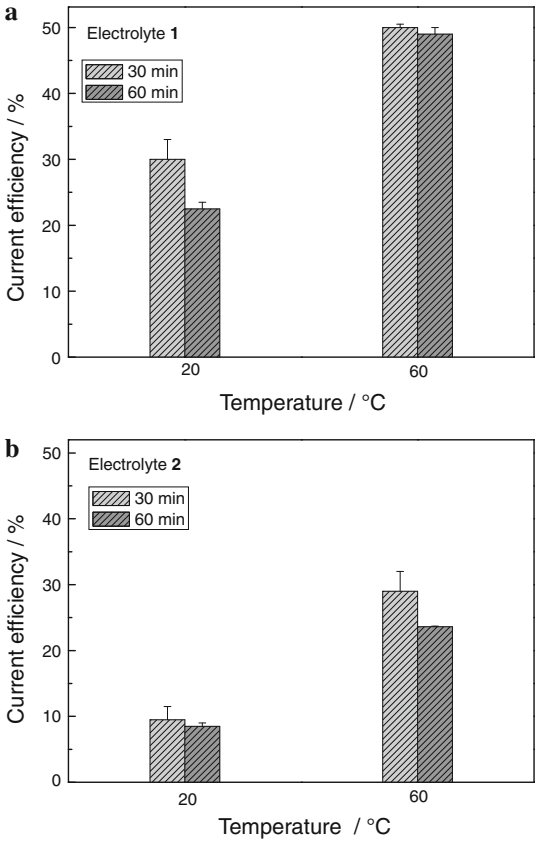

Fig. 1 Current efficiency of Ni–W alloy coatings electrodeposited by DC from citrate type of electrolyte in dependence on temperature and time of electrolysis for **a** Electrolyte 1 and **b** Electrolyte 2

Table 1 Composition of the electrolytes used for electrodeposition of Ni–W coatings

Electrolyte composition/mol dm^{-3}	$NiSO_4 \cdot 7H_2O$	$Na_2WO_4 \cdot 2H_2O$	Citric acid
Electrolyte **1**	0.071	0.242	0.238
Electrolyte **2**	0.071	0.500	0.238

reached for the coatings deposited from E1 electrolyte. In this case the higher content of the tungstate in the electrolytes prevents nickel electrodeposition (Table 1). Concerning the *pulse current* electrodeposition at the constant duty cycle and keeping the ratio t_{on}: t_{off} constant with changing *frequency,* it is clear that the shorter difference between time off and time on the current efficiency of the process is higher (Fig. 2). This could be explained by t_{off} that is sufficient enough for desorption and following nucleation [13]. Longer relaxing time triggers other reactions which in turn negatively affect the current efficiency of the process (hydrogen evolution).

Current efficiencies reach comparable values for DC and PC (active time 1 ms and constant duty cycle 9.1%) electrodeposition carried out in E1 (Fig. 3).

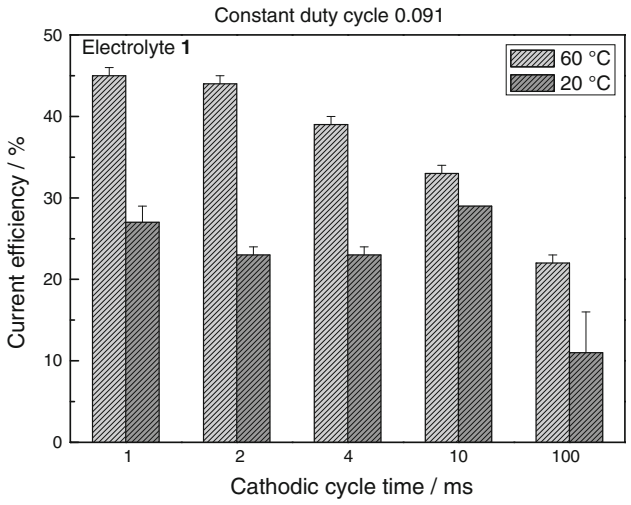

Fig. 2 Current efficiency of Ni–W alloy coatings electrodeposited by PC from citrate type of electrolyte in dependance on time of cathodic cycle (active time) for Electrolyte 1

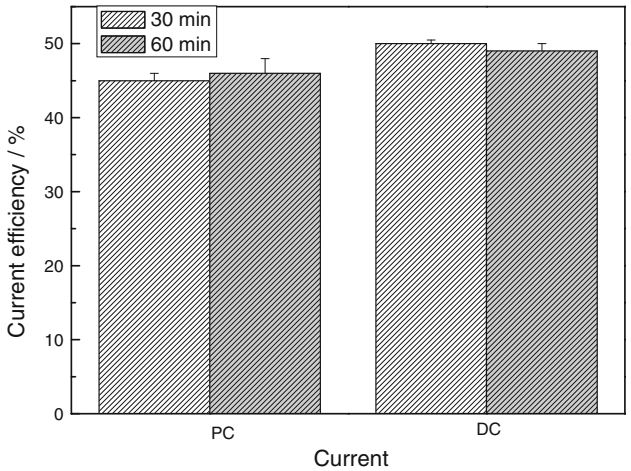

Fig. 3 Comparison of current efficiencies for Ni–W alloy coatings electrodeposited by PC and PC from citrate type of electrolyte at different time of electrodeposition

EDX analysis proved that the amount of nickel and tungsten in the analysed alloy coatings is comparable for DC and PC electrodeposition at the tested conditions (Table 2). The temperature influence on the amount of analysed elements is negligible. The essential influence on the amount of the analysed elements has an applied electrolyte composition. An elevated concentration of tungstate results in an increased amount of tungsten in the deposit.

Figure 4 shows the influence of the applied frequency on the morphology of the coatings. The coatings were recorded for the samples electrodeposited from E1 at different frequencies and a constant duty cycle. One can see the transition from the homogenous soft crystallite surface (a) to the swells with crystallites (b, c, d) till the smooth

Table 2 Content of Ni and W in Ni–W alloy coatings determined by EDX analysis

Electrodeposition condition	Ni/at.% 20 °C	W/at.% 20 °C	Ni/at.% 60 °C	W/at.% 60 °C
Direct current electrolyte **1**	83	5	87	11
Direct current electrolyte **2**	72	22	72	26
Pulse current (1:10) electrolyte **1**	80	17	85	13
Pulse current (1:10) electrolyte **2**	69	26	70	27

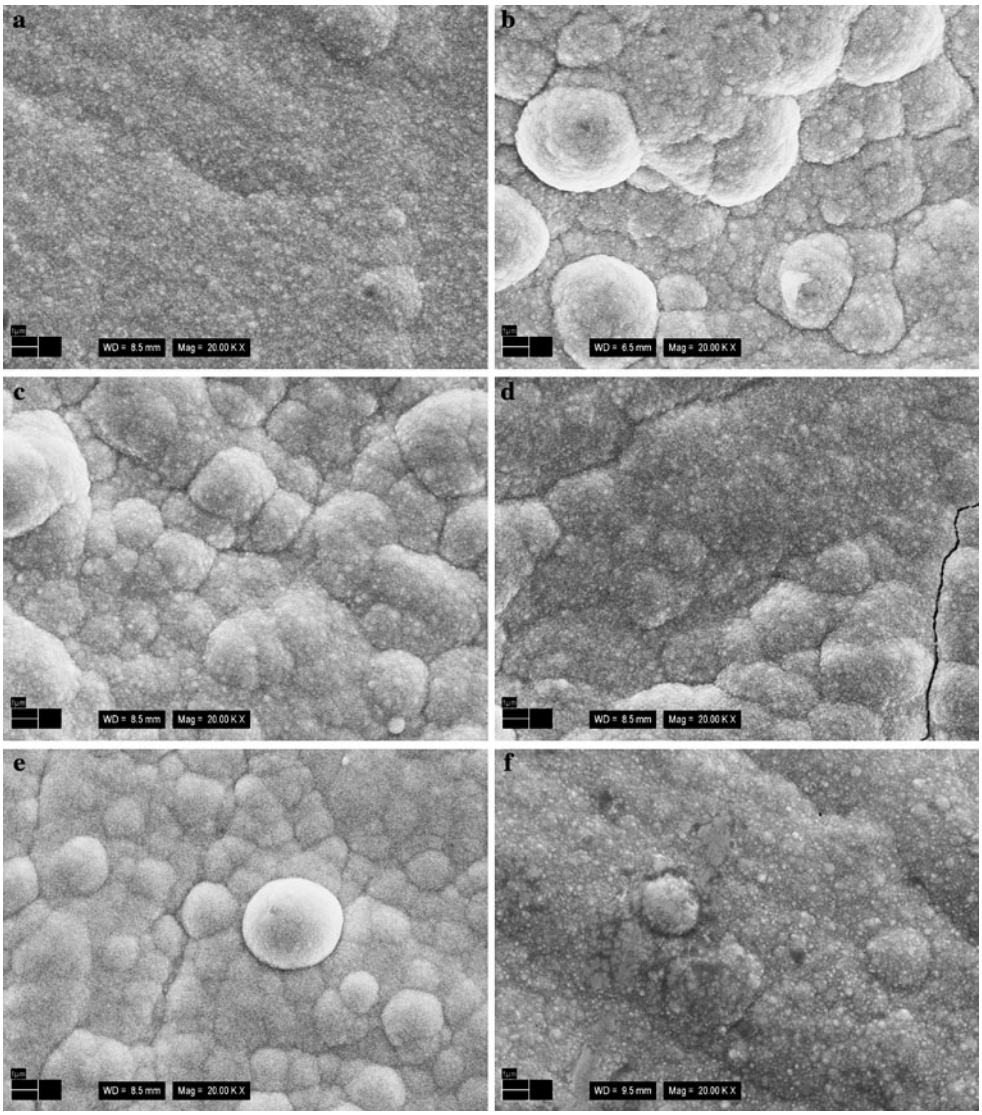

Fig. 4 SEM micrographs of the coatings prepared with usage of PC keeping constant duty cycle 9.1% at time of cathodic cycle **a** 1 ms, **b** 2 ms, **c** 4 ms, **d** 10 ms, **e** 100 ms and with usage of **f** DC

swell surface is formed (e). The swells with the crystallites on their surface appear with longer off time. A smooth swell surface arises with off time 100 ms. It can be seen that the morphology of the formed coating pictured in the micrograph (a) is similar to the one prepared by means of DC (f). This morphology is a relief one in comparison to the morphology of the coating shown in Fig. 4 micrograph (a). The morphology of the Ni–W alloy coating prepared by PC with cathodic cycle 1 ms and constant duty cycle 9.1% from E1 is the homogenous and regular one with a grain size down to some tenths of nm. *The SEM micrographs clearly confirm the influence of the PC frequency on the morphology of the coating*. If the pulse off-time is considered as the period when surface diffusion takes

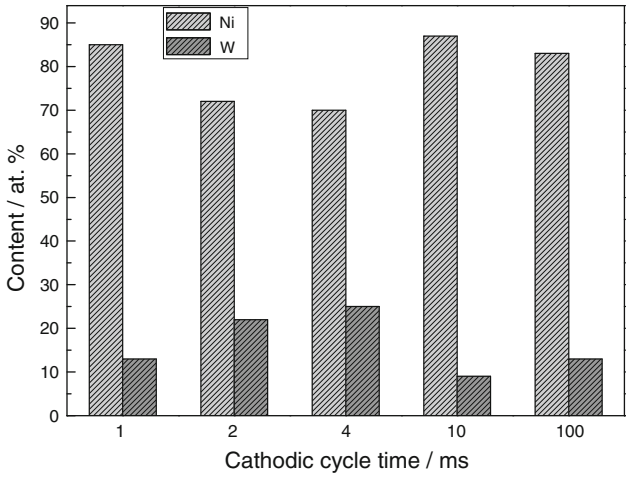

Fig. 5 Ni and W content obtained by EDX at different frequencies of PC Ni–W alloy coating electrodeposition

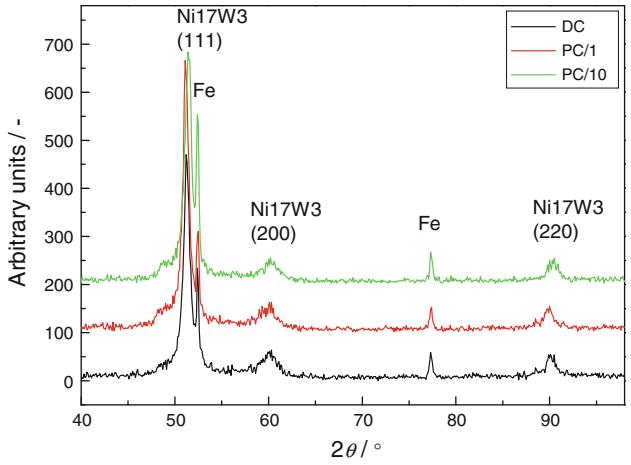

Fig. 6 XRD pattern of Ni–W metallic coatings deposited with usage of PC and DC from Electrolyte 1 at 60 °C, respectively

place, one can expect the re-arrangement of atoms and nuclei which may induce re-crystallization and hence an increase in the grain size. Generally, an increase in off-time results in an increase in grain size according to the processes related to re-crystallization as bigger grains are thermodynamically more stable than the small ones [14]. Small grains on the cavities reveal a re-crystallization process and imply the function of a complexing agent (citric acid) where previously absorbed Ni and W citric complexes are thought to block the growth centres of Ni and W during the off-time retaining diffusion [15]. Therefore for the next pulse new nuclei form resulting in a smaller grain size and granulating structure of the coating.

Tungsten content in the alloy coating is comparable for the samples prepared with cathodic cycle time 1, 10 and 100 ms. The tungsten content is above 20 at.% for samples prepared with cathodic cycle time 2 ms, 4 ms as one can see in Fig. 5.

On the basis of these results the following coating study and corrosion tests were carried out mainly on the samples deposited at active time 1 ms and constant duty cycle 9.1%.

The compact polycrystalline samples of Ni–W alloy coatings were examined by XRPD measurements. The powder patterns of the selected samples are presented in Fig. 6. Qualitative phase analysis reveals three peaks at 51, 60 and 90° 2θ in the diffractograms of Ni–W coatings related to the $Ni_{17}W_3$ phase. The $Ni_{17}W_3$ phase was also confirmed by the calculation of tungsten content in the compound using Vegard's law [16]. The calculated values are presented in Table 3. Lattice parameters of the electrodeposited subject were obtained with the programme of Laugier et al. [17]. The calculated values of Ni–W coating composition are in a good agreement with the composition of $Ni_{17}W_3$ phase given in ICSD database (ICSD # No 105454, Karlsruhe, Germany). Especially the coatings formed by pulse current at 1:10 conditions satisfied the Ni0.85W0.15 phase in the database that means phase $Ni_{17}W_3$ (Fig. 7).

Table 3 Identification of the studied NiW alloy coatings subject to electrodeposition conditions

Type of preparation	2θ/°	Lattice parameter/Å	Tungsten content/%
DCNiW60	51.274	3.58(3)	12
	59.900		
	90.150		
PCNiW1:10	51.174	3.59(3)	14
	59.687		
	89.872		
PCNiW10:100	51.420	3.57(1)	10
	60.106		
	90.368		

The peaks at 2θ angles about 54 and 78°are related to iron in the mild steel substrate. The selected samples (DC and PC electrodeposition from E1 at 60 °C; active time for PC electrodeposition 1 and 10 ms, respectively) have the same phase composition. The phase with the chemical composition $Ni_{17}W_3$, which crystallizes in the cubic crystallographic system was analysed on the surface of mild steel material. The corresponding Miller indices and crystallite size are introduced in Table 4, respectively. Full width at half maximum (FWHM) was determined by software *fityk* [18, 19]. One can see from the analysed results that alloy coatings prepared with cathodic cycle 1 and 10 ms and by means of DC reach about a tenth nm, the results confirming the crystallite size assumption taken from SEM micrographs. This analysis suggests that the W co deposited with Ni from this type of bath is only

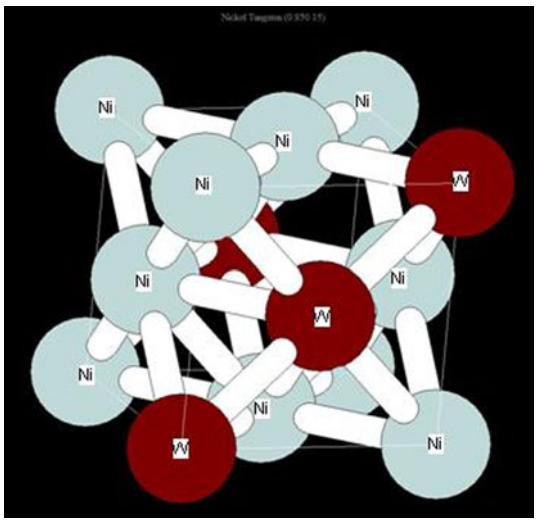

Fig. 7 Crystal structure of the $Ni_{17}W_3$ phase

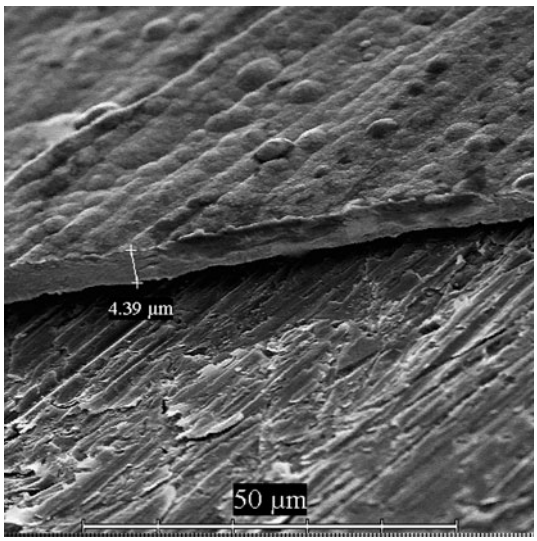

Fig. 8 Thickness of Ni–W alloy coating deposited from Electrolyte 1 by DC at 60 °C for 60 min deposition time

Table 4 Crystallite size of the studied NiW alloy coatings subject to electrodeposition conditions

Type of preparation	Diffraction indices	Crystallite size/nm
DCNiW60	111	21
	200	10
	220	18
PCNiW1:10	111	27
	200	8
	220	19
PCNiW10:100	111	23
	200	11
	220	21

deposited in its metallic form. Sridhar [20] first analysed a diffraction peak at 50.4° in the diffractograms as deposited coatings. The peak was related to the Ni_4W phase. The presence of this phase with low tungsten content was explained by the combination of quite low current density and high (50 °C) temperature of electrolysis. The same explanation could be used for the presented results. There are reports in the literature for electrodeposited Ni–W coatings suggesting tungsten atoms substitutionally dissolved in nickel with XRPD patterns suggesting that Ni–W alloy coating consisting of two phases amorphous and crystalline [6, 21]. Yamasaki integrates the amorphous phase formation with the tungsten content over 20 at.% in the alloy coating [22]. At the studied conditions just crystalline phase was recorded on the studied samples deposited from E1 and E2 electrolytes.

The thickness of the layer was measured on a cross section using SEM as well (Fig. 8). The coating thickness for 60 min DC electrodeposition is about 5 µm and for 30 min electrodeposition is about 2 µm.

3.2 Corrosion study

Selected Ni–W samples as mentioned above were chosen as a representative for corrosion studies. Moreover samples deposited by PC from E2 at the studied parameters were investigated as well. Ni–W coatings were investigated in the determined time intervals during a 500 h immersion test. Before each experiment, the steady state open circuit potential was obtained first then potentiodynamic cathodic and anodic polarization curves were acquired. From Tafel curves polarization resistance was determined following the calculation of the corrosion rate. Figure 9a shows the dependence of the open circuit potential E_{oc} on immersion time for samples electrodeposited from E1 by PC at the tested conditions. It is clearly seen that after 24 h when the E_{oc} potential slowly decreases, a corrosion process starts. Within 24 h immersion time the potential oscillates at a value of about $E_{oc} = -0.52$ V. Similar behaviour was reached for samples deposited by DC from E1. Figure 9b depicts the dependence of the sample weight on immersion time during testing in 6 wt% NaCl solution for the samples electrodeposited from E2 at time of cathodic cycle 1 ms and temperature 60 °C. One can see that during testing the sample weight remains almost constant. It follows passivation of the coating occurs. The samples electrodeposited from E1 show different behaviour. The weight of the analysed sample is continuously decreasing. Figure 10 shows the dependence of the corrosion rate on the immersion time for the selected samples. Generally, corrosion rates of the analysed coatings are comparable; the

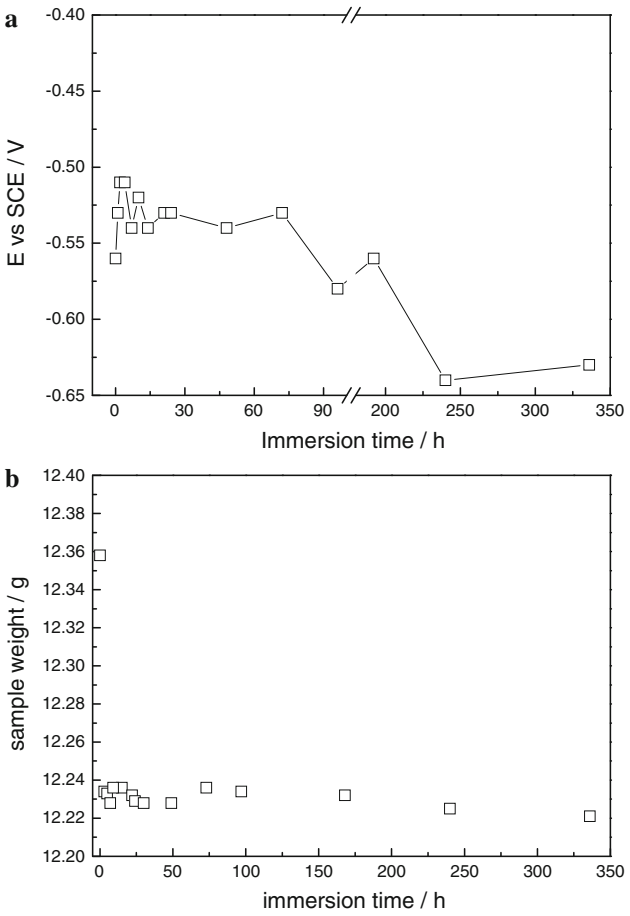

Fig. 9 Change of **a** the open circuit potential in dependence on immersion time and **b** the sample weight in dependence on immersion time in 6 wt% NaCl solution

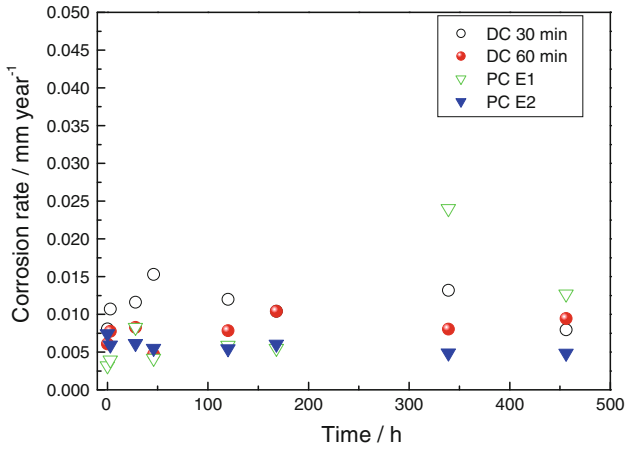

Fig. 10 Corrosion rate of the Ni–W alloy coatings in dependence on testing time in 6 wt% NaCl solution

corrosion rate of Ni–W coatings deposited from E2 electrolyte by PC with active time 1 ms and duty cycle 9.1% remains almost constant. The coatings deposited by DC corrode with nearly constant corrosion rate. The coatings

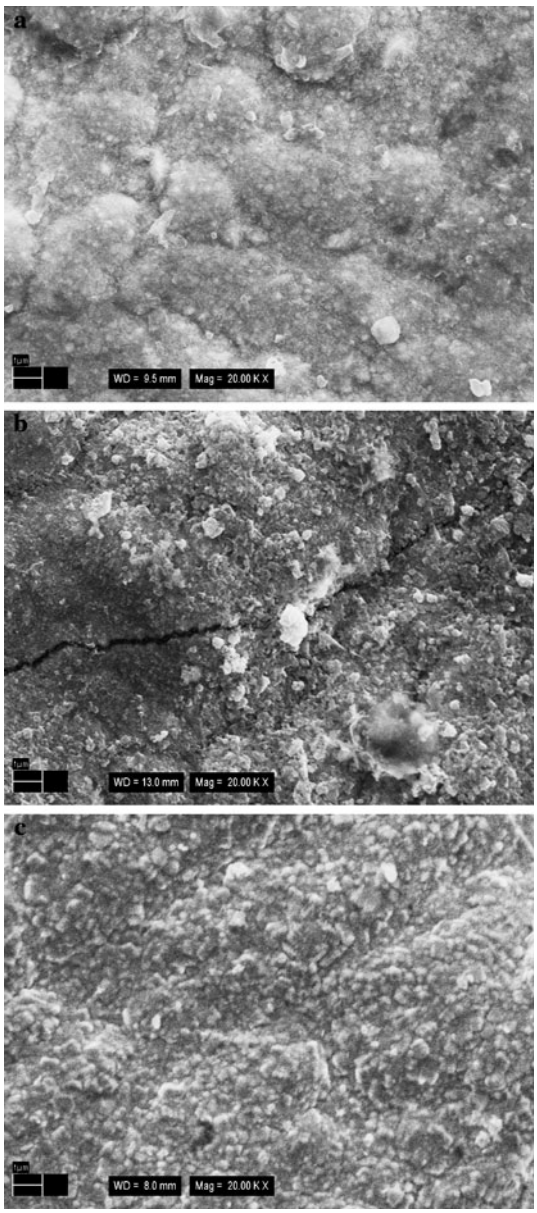

Fig. 11 SEM micrographs of Ni–W coatings after 500 h immersion time deposited **a** by DC from E1, **b** by PC from E1, and **c** by PC from E2

with a higher thickness (deposited at 60 min deposition time) provide a lower corrosion rate in chloride medium in comparison to the coatings deposited at the same conditions at 30 min deposition time. The coatings deposited by PC from E1 electrolyte at constant duty cycle 9.1% and active time 1 ms corrode rapidly after 300 h immersion time. One can conclude that homogenous nanocrystallite morphology of the coatings negatively contributes to the corrosion resistance of Ni–W coatings. Kabi et al. [23] found out that the lowest grain size and highest percentage of W provide the lowest corrosion resistance. Alimadadi et al. [24] on the other hand claims that nanocrystalline

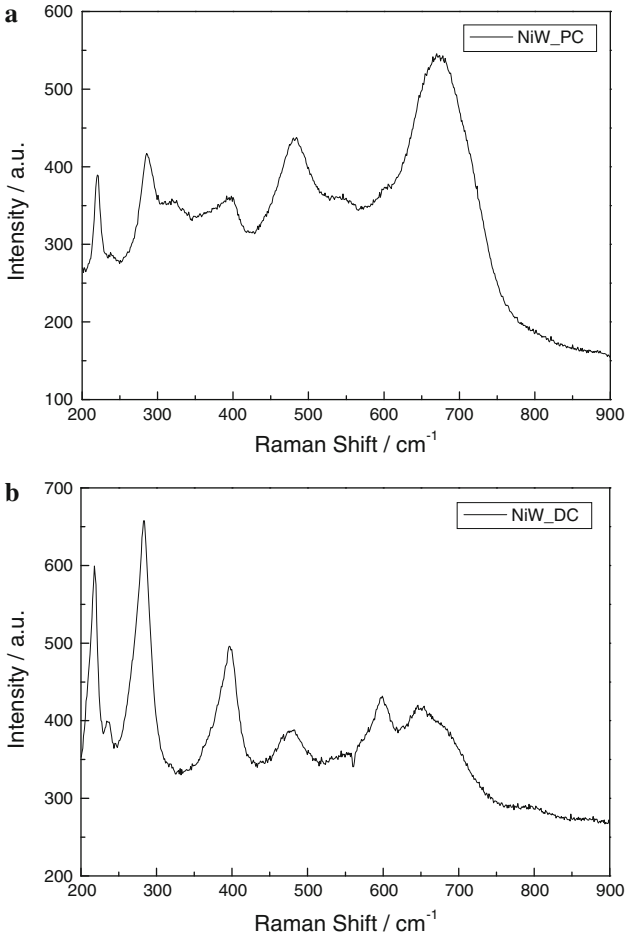

Fig. 12 Raman spectra of corrosion products after 500 h corrosion study on Ni–W alloy coatings deposited by **a** DC and **b** PC

Ni–W alloy comprising the highest amount of tungsten has the best anti-corrosion properties. Both studies were realized on copper substrate with electrolyte containing a citrate compound. These results confirm the sensitivity of Ni–W electrodeposition to the provided conditions of electrolysis. As one can see in Fig. 11 the morphology of the studied coatings after corrosion is degraded by corrosion products except the coatings deposited from E2 electrolyte by PC.

Raman spectra were collected to identify corrosion products formed on Ni–W surfaces during the immersion tests. Figure 12 shows the ex-situ Raman spectra of the corrosion products for Ni–W alloy coatings deposited from E1 electrolyte by PC with active time 1 ms and duty cycle 9.1%. Before corrosion noise is detected indicating Ni–W alloy coating in its metallic form. After corrosion in the middle of the sample no spectra could be collected. The corrosion products were identified in the edges of the tested samples. Consequently the corrosion of the coatings is non-homogeneous and non-regular. As one can see from Table 5 rust was identified as a product consisting of oxide-hydroxides of iron from the substrate [25]. The peak

Table 5 Location of Raman-active vibrational modes on the analysed Ni–W coatings

Band (cm^{-1})	Compound
220	alfa-Fe_2O_3
286	alfa-Fe_2O_3
394	FeOOH
482	NiO(OH)
602	Fe_2O_3
650	Fe_3O_4

observed at about 482 cm^{-1} is attributable to the NiO–OH stretching mode [25, 26]. One can conclude that preferential dissolution of nickel in the alloy coating occurs forming an area of a substrate corrosion attack. This fact is explainable by the degradation of nickel and its dissolution in the chloride solution. As the coating contains the metallic phase $Ni_{17}W_3$ and the potential of nickel is lower in comparison to tungsten, it is obvious that preferential dissolution of nickel in the alloy coating Ni–W occurs. These results are in good agreement with the work of Sriraman et al. [27].

4 Conclusion

Ni–W alloy coatings were prepared by PC electrodeposition changing frequency and keeping duty cycle constant. The prepared coatings were compared to those ones prepared by DC electrodeposition at the constant charge of the process. The stress was applied upon analysis of the coatings deposited at the determined conditions of electrodeposition (using electrolyte with lower concentration of tungstate, constant duty cycle and ratio of time on and time off, active time 1 ms). The new compound $Ni_{17}W_3$ was identified at the studied conditions. The corrosion rate of the nanocrystalline coatings prepared at the presented conditions is comparable to those prepared by DC. However, after 300 h the corrosion rate rapidly increases. Positive influence in terms of corrosion resistance of higher tungsten content in the Ni–W alloy coating was confirmed.

Acknowledgement The financial support of the Slovak Grant Agency research projects 1/0535/08 and 1/0579/10 is greatly acknowledged. M. Zemanová appreciates proof reading by K. Boehling (TU Darmstadt).

References

1. Brenner A (1963) Electrodeposition of alloys, vol II. Academic Press, New York
2. Eliaz N, Shridhar TM, Gileadi E (2005) Electrochim Acta 50:2893

3. Obradovic MD, Bošnjakov GŽ, Stevanovic RM, Maksimovic MD, Despic AR (2006) Surf Coat Technol 200:4201
4. Gáliková Z, Danielik V, Chovancová M (2006) Chem Pap 60:353
5. Krishnan RM, Kennedy CJ, Jayakrishnan S, Sriveeraraghavan S, Natarajan SR, Venkatakrishnan PG (1995) Met Finish 93:33
6. Slavcheva E, Mokwa W, Schnakenberg F (2005) Electrochim Acta 50:5573
7. de Lima P, Correia AN, Santana RAC, Colares RP, Barros EB, Casciano PNS, Vaz GL (2010) Electrochim Acta 55:2078
8. Atanassov N, Gencheva K, Bratoeva M (1997) Plat Surf Finish 84:67
9. Yao S, Zhao S, Guo H, Kowaka M (1996) Corrosion 52:183
10. Klug HP, Alexander L (1980) X-Ray procedures for polycrystalline and amorphous materials. Wiley/Interscience, New York
11. Bard AJ, Faulkner LR (2001) Electrochemical methods. John Wiley and Sons, New York
12. Joska L, Novák P (2001) Polarization resistance. In: Proceedings from II. International conference corrosion and influence on steel constructions. Tlačiareň Brno, Brno
13. Landolt D, Marlot A (2003) Surf Coat Technol 169–170:8
14. Puippe JC, Leaman F (1986) Theory and practise of pulse plating. American Electroplaters and Surface Finishers Soc, Orlando
15. Tury B, Lakatos-Varsanyi M, Roy S (2006) Surf Coat Technol 200:6713
16. Juškenas R, Valsiunas I, Pakštas V, Giraitis R (2009) Electrochim Acta 54:2616
17. Laugier J, Bochu B (2000) LMGP-suite suite of programs for the interpretation of X-ray experiments. ENSP/Laboratoire des Matériaux et du Génie Physique, Saint Martin d'Héres
18. Wojdyr M (2010) J Appl Cryst 43:1126
19. http://fityk.nieto.pl/
20. Sridhar TM, Eliaz N, Gileadi E (2005) Electrochem Solid State Lett C58:8
21. Juškenas R, Valsiunas I, Pakštas V, Selskis A, Jasulaitiene V, Karpavičiene V, Kapočius V (2006) Appl Surf Sci 253:1435
22. Yamasaki T, Tomohira R, Ogino Y, Schlossmacher P, Ehrlich K (2000) Plat Surf Finish 87:148
23. Kabi S, Raeissi K, Saatchi A (2009) J Appl Electrochem 39:1279
24. Alimadadi H, Ahmadi M, Aliofkhazraei M, Younesi SR (2009) Mater Des 30:1356
25. Oblonsky LJ, Devine TM (1995) Corros Sci 37:17
26. Lillard RS, Kanner GS, Daemen LL (2002) Electrochim Acta 47:2473
27. Sriraman KR, Raman SGS, Seshadri E (2007) Mater Sci Eng 460–461:39